Preparation of g-C_3N_4/$AgIn(MoO_4)_2$ and its photocatalytic degradation of tetracycline hydrochloride

Lijun Jia[1,a], Qianqian Zhang[1,b], Xu Yan[2,c], Ke Zeng[3,d*]

[1]School of Ecology and Environment, Zhengzhou University, Zhengzhou, Henan, China
[1]School of Ecology and Environment, Zhengzhou University, Zhengzhou, Henan, China
[2]School of Municipal and Environmental Engineering, Henan University of Urban Construction, Pingdingshan, Henan, China
[3]School of Hydraulic Science and Engineering, Zhengzhou University, Zhengzhou, Henan, China

Abstract: Graphite phased carbon nitride and indium silver molybdate [g-C_3N_4 / $AgIn(MoO_4)_2$]photocatalytic materials were prepared by hydrothermal method. X-ray diffraction, transmission electron microscope, scanning electron microscope, X-ray photoelectric spectrum, UV-vis diffuse reflection spectrum and solid fluorescence were used to analyze its structure and morphology. The results showed that the catalytic activity of g-C_3N_4 / $AgIn(MoO_4)_2$ was significantly higher than that of pure g-C_3N_4 and $AgIn(MoO_4)_2$ under visible light irradiation. Under the conditions of g-C_3N_4 and $AgIn(MoO_4)_2$ with a compound ratio of 2:1 and hydrothermal reaction at 120℃ for 6 hours, the degradation efficiency of tetracycline hydrochloride was the best. After 1 hour of light reaction, the degradation rate of tetracycline hydrochloride could reach 75.3%. g-C_3N_4/$AgIn(MoO_4)_2$ is expected to be a promising photocatalyst for wastewater treatment.

1 Introduction

Tetracycline hydrochloride (TC) is a biosynthetic broad-spectrum antibiotic, which is easily soluble in water and difficult to degrade. It is widely used in medical, livestock and aquaculture industries[1]. Compared with other types of industrial wastewater, antibiotic wastewater has the characteristics of complex composition, high concentration of organic matter and poor biodegradability, which is difficult to treat[2]. At present, TC levels of different concentrations of various water environments in China are detected[3]. The results showed that tetracycline antibiotics were highly concentrated in winter, and relatively low in summer. It is about 19.15-147.15ng/L in winter and 5.61-63.26ng/L in summer.This may be caused by high incidence rate of diseases in winter.

In photocatalysis, semiconductors are often used as photocatalytic materiasl because of their unique band structure[4]. Photocatalysis technology has the characteristics of high degradation efficiency, simple operation, no secondary pollution and direct use of sunlight, which shows a good application prospected for the treatment of wastewater containing TC[5].

In 2009, when g-C_3N_4 photocatalyst was used by Wang Xinchen[6] and others as photocatalyst, it was found that g-C_3N_4 had higher photolysis activity of aquatic hydrogen under visible light. Since then, the study of g-C_3N_4 photocatalysis materials has been launched around the world. g-C_3N_4 has a suitable band gap of about 2.7eV, which is characterized by visible light response, non-toxic and easy preparation[7、8、9]. Therefore, it is widely used in the field of photocatalysis, including photocatalytic degradation of pollutants, catalytic organic reactions and photolysis of water to produce hydrogen and oxygen[10]. Although g-C_3N_4 photocatalyst has a good application for the field of photocatalysis, it is difficult to be applied in practice because of its small specific surface area, which leads to the recombination problem of photogenerated carriers in the process of surface or internal migration. A large number of researchers have done research on the modification of g-C_3N_4, including regulating the preparation process of g-C_3N_4[11、12、13], and building heterojunction by combining other semiconductors and g-C_3N_4[14、15、16]. In this paper, g-C_3N_4 was compounded with a kind of material and its photocatalytic properties were studied. As a bimetallic molybdate, $AgIn(MoO_4)_2$ has good electrical and optical properties, and can be excited by visible light. It is an ideal visible light response photocatalyst[17]. Therefore, the photocatalytic properties of g-c3n4 and $AgIn(MoO_4)_2$ were studied.

2 Test

2.1 Reagents and instruments

Reagent : 99.5%melamine、99.9%Indium nitrate、99.8%silver nitrate、99.0%Sodium molybdate、99.0%Tetracycline hydrochloride.

Instrument : X-ray diffractometer (Bmker-DS

[a]email: jlj54254586@163.com, [b]email: zqq1524978@163.com, [c]email: yanxu123987@163.com
[*]Corresponding author:[d]email: zengke@zzu.edu.cn

Advance, Brooke company); Field emission scanning (Quanta FEG 250, FEI company）;electron microscope Field emission transmission (Tecnai G2 F20,FEI company); Field emission transmission electron microscopy

X-ray photoelectron spectrometer (Thermo Fisher K-AlpHa, Thermo air Inc); UV-Vis diffuse reflectance spectrometer (Hitachi UV-3150, Hitachi Japan); Fluorescence spectrophotometer (Hitachi F-4500,Hitachi Japan); Ultraviolet visible spectrophotometer (UV-5800PC, Shanghai yuananalytical Instrument Co., Ltd); Ma Fulu (JK-SX2-5-12N, Shanghai Jingxue Scientific Instrument Co., Ltd); Electric blast drying oven (101-2B, Beijing Hengnuo Lixing Technology Co., Ltd); High speed centrifuge (TGL-16C, Jiangsu Zhongda Instrument Technology Co., Ltd); Analytical balance (AB204-N, Shanghai Zesheng Technology Co., Ltd).

2.2 Preparation of catalyst

2.2.1 Preparation of g-C_3N_4

Take appropriate amount of melamine, grind up 5-10 min, raise the temperature to 500 ℃ in a furnace at the rate of 2 ℃ / min, react for 0.5 h, then raise the temperature to 550 ℃, react to 3 h, and finally naturally cool to room temperature. Then the obtained powder samples were centrifugally cleaned, and the pH value of the cleaning supernatant was placed in the drying box after 6-7, and dried at 60 ℃, and the light yellow powder obtained was g-C_3N_4.

2.2.2 Preparation of $AgIn(MoO_4)_2$

$AgIn(MoO_4)_2$ was prepared by hydrothermal method. $AgNO_3$ 0.084g, 0.5mmol and $In(NO_3)_2$ 0.150g, 0.5mmol were dissolved in 10ml deionized water, ultrasonic for about 3-5min, stirring vigorously for 15min, 10ml0.1M was added Na_2MoO_4 solution was added to the above solution drop by drop, and the ultrasonic stirring was continued for half an hour. Then, the pH value was adjusted to about 5 with NaOH and HNO_3 solutions, and the stirring was continued for 20 mins. The obtained mixed solution is heated in an electric oven for hydrothermal reaction to 180 ℃ for 24h, and then cool naturally; the supernatant in the reactor is poured out, and the orange yellow precipitate left at the bottom of the reactor is washed with deionized water and absolute ethanol until the pH value of the supernatant is 7; finally, the obtained sample is dried at 60 ℃.

2.2.3 Preparation of g-C_3N_4/$AgIn(MoO_4)_2$

The composite photocatalysis materials were prepared by hydrothermal method. A certain mass of g-C_3N_4 and $AgIn(MoO_4)_2$ were dissolved in deionized water. After ultrasonic stirring for half an hour, the hydrothermal reaction was carried out at 120 ℃ for 6 hours. After the hydrothermal reactor was cool, deionized water and anhydrous ethanol were used for cleaning and drying. The results show that the mass ratio of g-C_3N_4 to $AgIn(MoO_4)_2$ is 1:1, 1:2, 2:1, 3:1 and 4:1.

2.3 Photocatalytic degradation of TC

The preparation of TC :Take 100mg tetracycline hydrochloride drug, dissolve it in deionized water, oscillate and ultrasound for several times to make it fully dissolve, transfer it to 1000mL volumetric flasks, constant volume to scale line, and keep it away from light.

Photocatalytic degradation of TC :Waged 100mg photocatalyst sample, placed it in the reactor, added 90mL of deionized water, ultrasonic for 3-5min, then took 10mL of TC solution with a concentration of 100mg/L, and continued to stir it in dark for half an hour to ensure that TC solution reached the adsorption-desorption equilibrium on the sample surface. After dark adsorption, the circulating water was turned on to maintain the temperature of the system and the xenon lamp was turned on at the same time. Samples were taken every 10 minutes, 10mL of each sample was sampled and placed away from light. Centrifugal separation was made between solid and liquid.

The photocatalytic activity of the samples was analyzed by simulating the concentration change of tetracycline hydrochloride under sunlight. The photocatalytic efficiency was expressed by C_t/C_0, C_0 was the initial concentration of TC, and C_t was the concentration of tetracycline hydrochloride after t time of photocatalytic degradation. The maximum absorption wavelength of tetracycline hydrochloride (TC) is 357 nm, and the calculation formula of photocatalytic efficiency is as follows:

$$DR = \frac{C_0 - C_t}{C_0} \quad (1)$$

3 Results and discussion

3.1 Catalyst characterization

3.1.1 XRD analysis

The structure and composition of g-C_3N_4, $AgIn(MoO_4)_2$ and g-C_3N_4/$AgIn(MoO_4)_2$ samples were analyzed by XRD.

In this experiment, when preparing $AgIn(MoO_4)_2$, the pH value of the solution was adjusted to 4.8, close to 5, because $AgIn(MoO_4)_2$ is easy to crystallize under acidic conditions. As shown in Fig. 1, the XRD pattern of g-C_3N_4 shows two obvious diffraction peak at 15 ° and 28 ° respectively. It can be seen from the XRD results that all the samples contain the diffraction peak of $AgIn(MoO_4)_2$(JCPDS No.36-0312), and there are obvious characteristic peaks at 20°and 28°in the 1:1 composite sample, and obvious characteristic peak at 28° and 30°in the 2:1, 3:1, 4:1, 5:1 composite samples, and the intensity of the characteristic peak is the highest at 2:1.

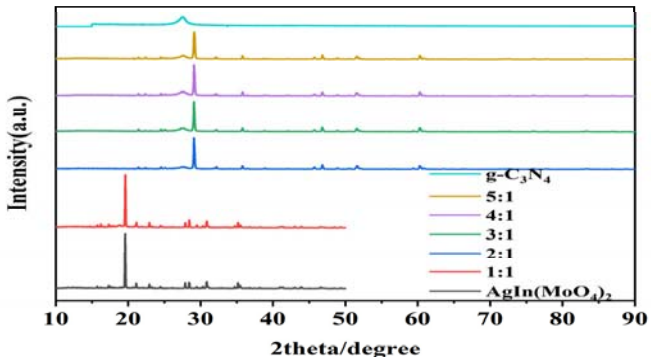

Fig. 1 XRD spectrum of the prepared catalyst

3.1.2 Analysis of SEM and TEM images

As shown in Fig. 2(a) and (b), g-C_3N_4 presents an irregular layered stacked plate particle structure, which is consistent with the structure of graphite-like phase. It can be seen in (c) what the morphology of $AgIn(MoO_4)_2$ is monodisperse nano flake, which is obvious. In (d) and (e), the surface of $AgIn(MoO_4)_2$ nano sheet is compounded with g-C_3N_4, which is an irregular layered stacking flat particle structure.

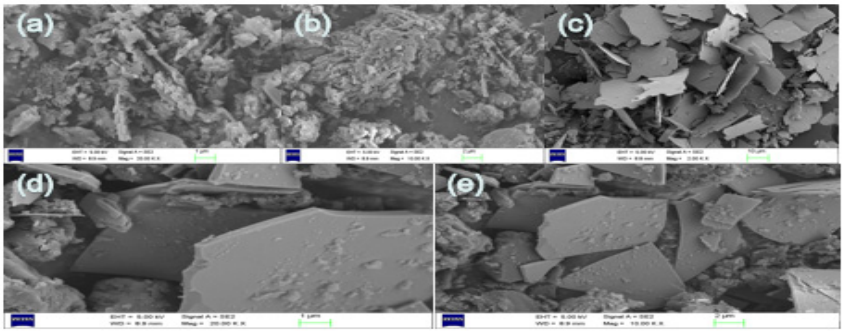

Fig. 2 SEM images of g-C_3N_4 (a), (b); SEM images of $AgIn(MoO_4)_2$ (c); SEM images of g-C_3N_4 / $AgIn(MoO_4)_2$ (d), (e)

The TEM of g-C_3N_4 / $AgIn(MoO_4)_2$ is shown in Fig. 3. According to the TEM test results, (a) and (b) can be clearly seen that there are lighter colored substances around the dark colored substances. In the SEM images, it is known that g-C_3N_4 is a stacked structure, $AgIn(MoO_4)_2$ is a sheet structure, and obviously, the darker material is $AgIn(MoO_4)_2$, and the lighter color is g-C_3N_4, so g-C_3N_4 was deposited on $AgIn(MoO_4)_2$ nanosheets.

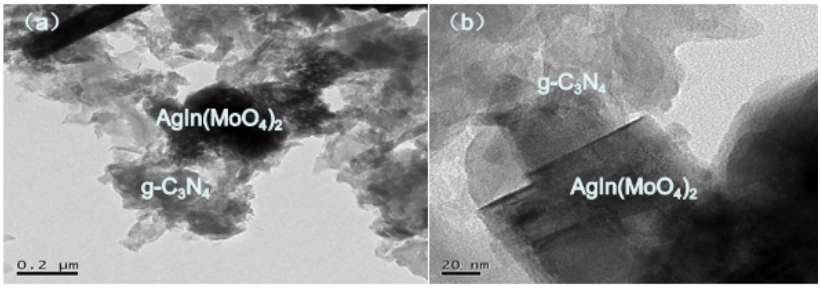

Fig. 3 TEM diagrams (a), (b) of g-C_3N_4/$AgIn(MoO_4)_2$

3.1.3 UV-vis absorption spectrum analysis

Fig. 4 shows the UV -Vis diffuse reflectance spectra of g-C_3N_4, $AgIn(MoO_4)_2$ and g-C_3N_4/$AgIn(MoO_4)_2$ samples.

According to the reflection in the figure, the absorption band edge of g-C_3N_4/$AgIn(MoO_4)_2$ sample is red shifted compared with that of pure $AgIn(MoO_4)_2$. In the visible light range, the light absorption intensity of the composite sample is significantly improved. Therefore, the utilization degree of visible light of g-C_3N_4/$AgIn(MoO_4)_2$ sample is improved, and the photocatalytic activity is enhanced compared with that of pure g-C_3N_4 and $AgIn(MoO_4)_2$.

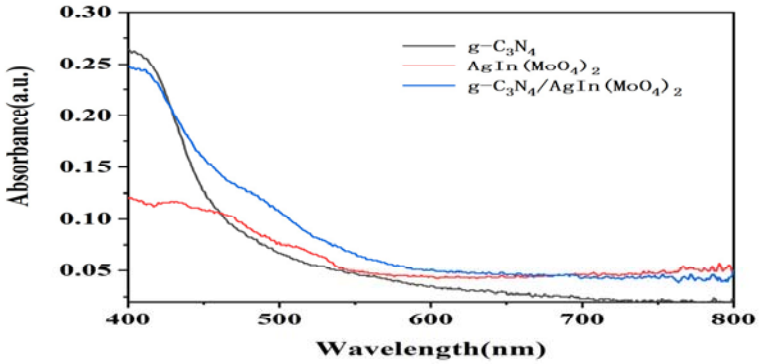

Fig. 4 UV -Vis diffuse reflectance spectrum

3.1.4 Analysis of XPS spectrum

As shown in Fig. 5 and Fig. 6, the spectra of g-C_3N_4/AgIn$(MoO_4)_2$ nano sheet photocatalyst are shown, which provides the structural information of the catalyst.

There are two XPS peaks at 367 and 373ev of Ag3d in Fig. 5, corresponding to the characteristic peaks of Ag3d in Fig. 6 (a), two XPS peaks at In3d spectral orbits 444.5 and 453ev, corresponding to In3d characteristic peaks in Fig. 6 (b), two XPS peaks at Mo3d spectral orbits 232.2 and 235ev in Fig. 5, corresponding to the characteristic peaks of Mo3d in Fig. 6 (c), and O1s spectral orbits in Fig. 5 There are two XPS peaks at 530 and 532.5ev, corresponding to the characteristic peaks of O1s in Fig. 6 (d), two XPS peaks at C1s spectral orbits 284.5 and 288.3ev in Fig. 5, corresponding to the characteristic peaks of C1s in Fig. 6 (e), respectively; XPS peaks at 399ev of N1s in Fig. 5 correspond to the characteristic peaks of N1s in Fig. 6 (f). Combined with the previous XRD patterns, these two spectra fully proved the successful preparation of g-C_3N_4/AgIn$(MoO_4)_2$ composite photocatalyst.

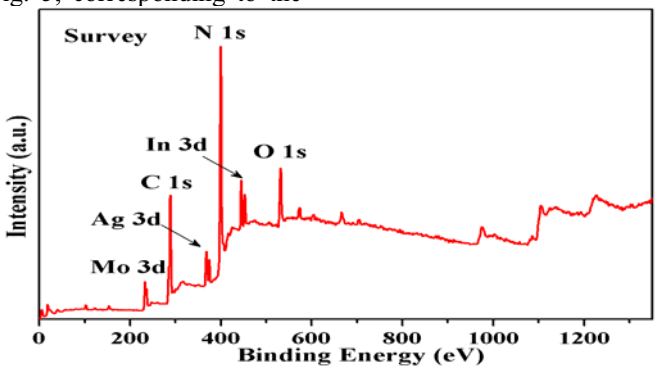

Fig. 5 g-C_3N_4/AgIn$(MoO_4)_2$ XPS spectrum

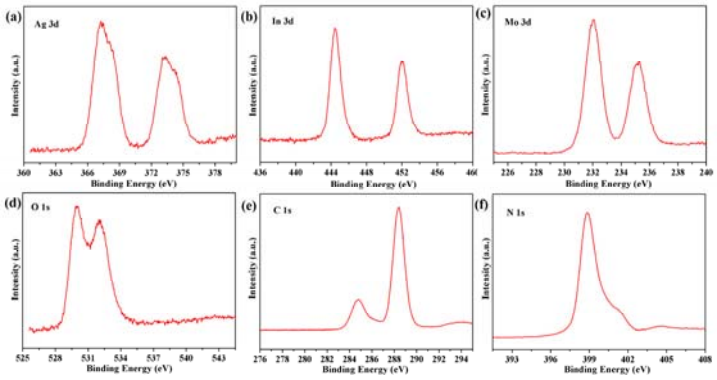

Fig. 6 g-C_3N_4/AgIn$(MoO_4)_2$ XPS combination diagram

3.2 Photocatalytic performance test

In this test, the photocatalytic activity of the photocatalyst was analyzed by the degradation test of TC.

As shown in Fig. 7, after one hour of photo reaction, each catalyst has certain degradation activity for TC. Among them, the photocatalytic activity of 2:1 g-C_3N_4/AgIn$(MoO_4)_2$ composite sample is the highest, and its degradation efficiency can reach 75.3%, while the degradation efficiency of pure g-C_3N_4 and AgIn$(MoO_4)_2$ samples is 64.3% and 43.4%, respectively. In this way, the degradation efficiency of g-C_3N_4 and AgIn$(MoO_4)_2$ samples is higher than that of pure g-C_3N_4 and AgIn$(MoO_4)_2$ samples.

The low degradation efficiency of pure g-C_3N_4 and AgIn$(MoO_4)_2$ samples may be due to the low absorption rate of visible light and the high recombination rate of photogenerated carriers. The reasons for the

improvement of photocatalytic activity are as follows: first, g-C_3N_4 can improve the light absorption rate of photocatalyst; second, the specific surface area of $AgIn(MoO_4)_2$ increases after the combination of g-C_3N_4 and $AgIn(MoO_4)_2$; thirdly, the valence band position of the two photocatalytic materials promotes the transfer of photogenerated carriers. However, excessive g-C_3N_4 on $AgIn(MoO_4)_2$ leads to the decrease of photocatalytic activity, which may be due to the influence of g-C_3N_4 on the visible light absorption of $AgIn(MoO_4)_2$, which directly affects the number of photogenerated electron hole pairs.

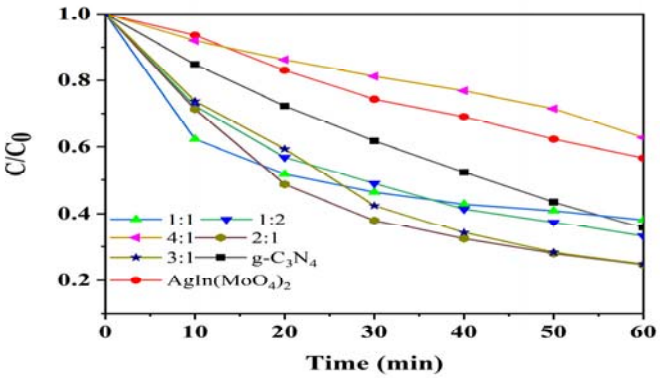

Fig. 7 experimental curves of TC degradation by different catalysts

3.3 Mechanism analysis of photocatalytic enhancement

3.3.1 PL spectrum analysis

The generation of fluorescence emission spectra comes from the recombination of carriers. As shown in Fig. 8, the fluorescence spectra of g-C_3N_4, $AgIn(MoO_4)_2$ and g-C_3N_4/$AgIn(MoO_4)_2$ samples are shown in Fig. 8. In the spectrum of g-C_3N_4 photocatalyst, the wide fluorescence emission peak occurs near the wavelength of 450nm, which is the band edge fluorescence phenomenon caused by light excitation. The intensity of fluorescence emission peak of g-C_3N_4/$AgIn(MoO_4)_2$ sample is obviously weaker than that of g-C_3N_4. The intensity of fluorescence emission peak reflects the recombination rate of photogenerated carriers to a certain extent. The decrease of emission peak intensity indicates that the recombination rate of photogenerated carriers in g-C_3N_4/$AgIn(MoO_4)_2$ sample is lower than that of g-C_3N_4. Therefore, the composite $AgIn(MoO_4)_2$ sample is conducive to the separation of photogenerated electron hole pairs, enhances the photocatalytic activity of the sample, and effectively inhibits the fluorescence characteristics of the photocatalytic material.

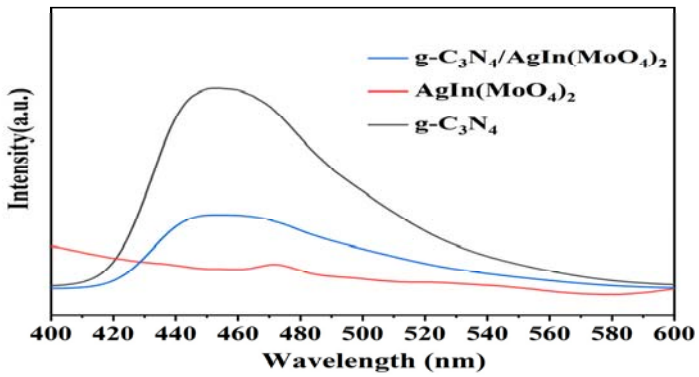

Fig. 8 fluorescence spectrum

3.3.2 Experimental analysis of active species capture

In order to explore the action mechanism of each active component in the reaction process, the action mechanism of each active component was explored by adding capture agent in the reaction process of different active components. Isopropanol (IPA) is used as ·OH capture agent, potassium dichromate is used to captured photo excited electrons, nitrogen is introduced to remove oxygen in water, so that electrons cannot react with oxygen to form superoxide radicals, and triethanolamine is used to capture photo excited holes.

As shown in Fig. 9, the results of active component capture experiment for visible light degradation of TC in composite samples with optimal ratio are shown in the figure. It can be seen from the figure that when triethanolamine is added during the experiment, TC almost does not degrade, which indicates that holes are important active components. When N_2 and $K_2Cr_2O_7$ were added into the reaction process, the degradation efficiency of TC decreased significantly compared with that without any capture agent, indicating that superoxide radicals and electrons are also important active

components. When isopropanol was added into the reaction as a capture agent, the degradation efficiency of TC also decreased, but the range was not too large, indicating that ·OH was not the main active component.

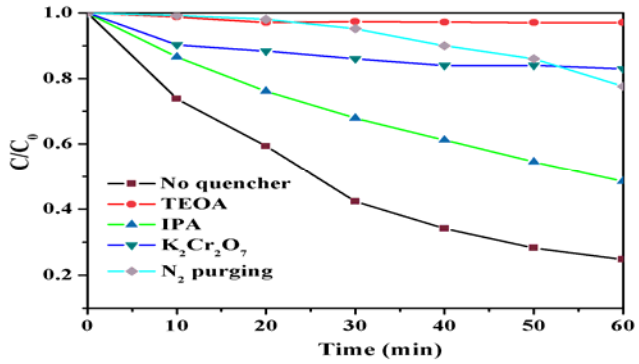

Fig. 9 the capture experimental degradation curve of TC in g-C_3N_4/AgIn$(MoO_4)_2$ under visible light

3.3.3 Photocatalytic enhancement mechanism of g-C_3N_4/AgIn$(MoO_4)_2$

The mechanism of photocatalytic degradation of TC by g-C_3N_4/AgIn$(MoO_4)_2$ is shown in Fig. 10. Under visible light irradiation, g-C_3N_4 and AgIn$(MoO_4)_2$ are simultaneously excited to produce electron-hole pairs. The holes in the valence band of g-C_3N_4 combine with the electrons in the conduction band of AgIn$(MoO_4)_2$. The electrons in the conduction band of g-C_3N_4 react with oxygen to form superoxide radicals. The holes in the valence band of AgIn$(MoO_4)_2$ react with water to form hydroxyl radicals, which can catalyze the oxidation of TC. According to the above analysis, electron conduction is a Z-scheme reaction mechanism in the photocatalytic degradation of TC by g-C_3N_4/AgIn$(MoO_4)_2$.

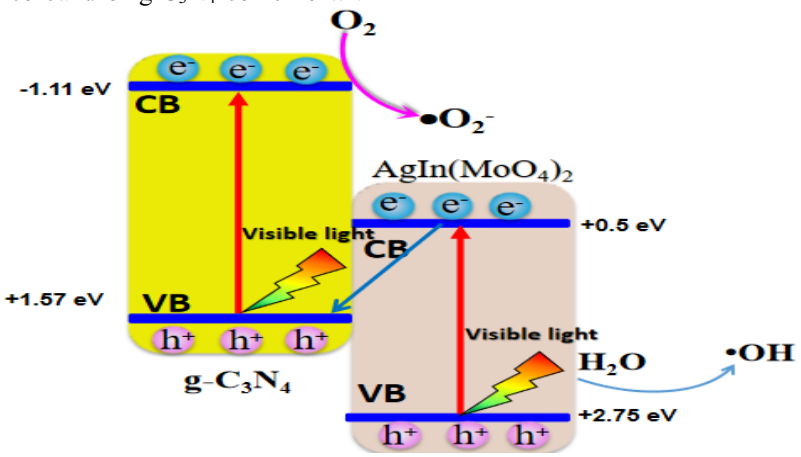

Fig. 10 pHotocatalytic reaction mechanism of g-C_3N_4/AgIn$(MoO_4)_2$

4 Conclusion

（1）Different proportions of g-C_3N_4/AgIn$(MoO_4)_2$ composite samples were synthesized by hydrothermal method. The structure and morphology of g-C_3N_4/AgIn$(MoO_4)_2$ catalyst was analyzed by XRD, SEM, TEM, XPS, UV-vis and PL.

（2）Taking TC as target pollutant, the activity of g-C_3N_4/AgIn$(MoO_4)_2$ catalyst was tested and analyzed under visible light irradiation. The maximum degradation rate of TC was 75.3% with the best proportion of sample, which was significantly higher than that of pure g-C_3N_4 and AgIn$(MoO_4)_2$ samples. The reason may be that the valence band position of the two photocatalytic materials promotes the transfer of photogenerated carriers after the combination of g-C_3N_4 and AgIn$(MoO_4)_2$, the specific surface area of AgIn$(MoO_4)_2$ was increased and more active sites were produced.

（3）g-C_3N_4/AgIn$(MoO_4)_2$ is expected to be a promising photocatalyst for wastewater treatment. Z reaction mechanism is a new method of the development of composite photocatalyst.

References

1. Zhang, YL., Wei, C., Sheng GS. (2020) Study on the degradation of tetracycline by visible light synergistic activation of BiFeO_3 persulfate . Guangzhou chemical,45:30-35.
2. Zhang, Y. (2018) Research progress of pharmaceutical wastewater treatment technology. Industrial water treatment,38:5-9.
3. Zhang, Q., Xin, Q., Zhu, JM., Cheng, JP. (2014) Current status of antibiotic pollution and its ecological and environmental effects in main waters of China. Environmental chemistry,33:1075-1083.

4. Wang, YJ. (2011) Study on improving photocatalytic performance of conjugated molecular surface hybridization. Tsinghua University.
5. Bu, D. (2017) Study on photocatalytic degradation of antibiotic wastewater [J]. Management and technology of small and medium-sized enterprises,138-140.
6. Wang, XC., Maeda, K., Thomas, A., et al. (2009) A metal-free polymeric photocatalyst for hydrogenproduction from water under visible light. Nature Materials, 76-79.
7. Chen, Y., Liu, HB. (2017) Construction of ultrathin graphite-phase carbon nitride nanosheets and their photocatalytic activity. Journal of Inorganic Chemistry,33:2255-2261.
8. FU J W,YU J G,JING C J,et al.(2018) G-C_3N_4-based heterostructured photocatalysts.Advanced Energy Materials,8:1701503.
9. NIU P,ZHANG L Z,GANG L,et al.(2012) Graphitic carbon nitride as a metal-free catalyst for NO decomposition.Chemical Communications,22:4763-4770.
10. Ma, YG., Guo, XF. (2018) Doping modification of carbon nitride and its photocatalytic performance. Materials Science and Engineering. Chongqing: Chongqing Jiaotong University.
11. Zhao Z L, Wang X L, Shu Z, et al. (2018) Applied Surface Science,455,591.
12. Liu C Y, Huang H W, Ye L Q, et al. (2017) Nano Energy,41,738.
13. Zhou C, Shi R, Shang L, et al. (2018) Nano Research,11,3462.
14. Yu W L, Chen J X, Shang T T, et al. (2017) Applied Catalysis:Environmental,219,693.
15. Di J, Xia J X,Yin S, et al. (2014) Journal of Materials Chemistry A,2,5340.
16. Han M M, Wang H B, Zhao S Q, et al. (2017) Inorganic Chemistry Frontiers,4,1691.
17. Yan, X, Shi, WD. (2018) Construction of heterophotocatalyst and its photodegradation performance of environmental pollutants. Clean energy and environmental protection. Zhenjiang: Jiangsu University.